Theoretical Study of band gap of $PbCrO_4$ under high pressure

DR. Pankaja Singh[1],Professor , Department of Physics, Govt.S V College Raisen

pankajasingh@gmail.com

Nikita Persai[2], Research Scholar, Department of Physics, MLBCollege Bhopal
nikita_persai@rediffmail.com

Abstract

Lead Chromate (**$PbCrO_4$**) is use as photo sensitizer and yellow pigment with a monoclinic P21/. Monoclinic structure, P21/n space group (monazite). A little-studied mineral need to explore. It is a structurally fine semiconductors have theoretical value Eg~ 2.2 eV. Band-structure calculations have been carried out up to 12 GPa. Calculations at higher pressures were not performed because the crystal structure of $PbCrO_4$ beyond 12 GPa remains yet undetermined. The band-structure calculations were performed within the framework of density-functional theory, using the plane-wave pseudo-potential method as implemented in the VASP package. The atomic species were described with projected-augmented wave (PAW) pseudo-potentials. The exchange-correlation energy was taken in the generalized-gradient approximation (GGA) with the PBE sol prescription

Introduction

In recent years, much attention has focused on nanostructured systems applied in electronic devices or to improve mechanical, chemical, structural, optical, electrical and magnetic properties of materials [1-2]. Manipulation of the thermodynamic and kinetic control processes plays a key role in crystal growth, which determines the final crystal habit, phase, shape, and structures [3-4]. The added value of a compound depends on its structural, morphological and optical properties. These properties

depend directly on the crystal structure of the material. Thus, studies relating to the material's structure, physical properties, and method of synthesis are essential.

Lead chromate ($PbCrO_4$) is an important solid material that is widely used as a photo sensitizer and yellow pigment with a monoclinic P21/n structure [5]. Pb_2CrO_5 was first used as a dielectric material in 1968[6]. Dileadpentaoxochromate (Pb_2CrO_5) with a monoclinic C2/m structure has a large absorption coefficient and a high-speed photo-response in the visible region of the electromagnetic spectrum. Therefore, it is a potential candidate for application in photoconductors, optoelectronic devices, and reversible thermochromism materials [7]. Pb_2CrO_5 has been found to have wide band gap energy ($E_g \sim$ 2.1-2.3 eV) and a large absorption coefficient ($\mu \sim 10^4$ cm$^{-1)}$. The photo response and performance of Pb_2CrO_5 devices described in the literature suggest that Pb_2CrO_5 may be classified as a new type of optoelectronic dielectric material that could potentially be used in room temperature photoconductors for the visible and ultraviolet regions [8]. The synthesis of $PbCrO_4$ and Pb_2CrO_5 crystals with well-controlled sizes and shapes is crucial due to their potential applications. The literature describes various procedures to synthesize $PbCrO_4$ and Pb_2CrO_5 crystalline phases into different shapes, such as spherical nanoparticles, nanorods, microparticles, nanowires, rectangular nanorods and nanotubes [9-15]. The reported methods are microemulsion[9], hydrothermal[11], self-seeding template growth (SSTG) process[12], microwave-assisted ionic liquid method, and room temperature reaction of solutions without the additives[14].

The polymeric precursor route, the Pechini method, is a nonconventional method of synthesis that offers the advantage of yielding homogeneous systems with a high degree of purity, which can be claimed at relatively low temperatures, allowing the synthesis of nanometric oxides with well defined and controlled properties.

In this work, $PbCrO_4$ and Pb_2CrO_5 crystalline particles, known as crocoites, were synthesized via a soft chemical route, the polymeric precursor method, and the structural, microstructural and optical properties of these crocoites annealed at different temperatures were examined to be used as pigments.

Lead chromate ($PbCrO_4$, "crocoite") is a mineral that crystallizes at ambient conditions in a monoclinic structure belonging to P 21/n space group (monazite structure) [4]. It is in some pyrotechnic compositions and as a pigment in some paints, because it is practically insoluble in water. It can also be used as a photocatalyst and has been proposed as a potential laser-host material. PbCrO4 is a

very toxic substance. It's quite rare in nature but it can be created in laboratory.X-ray diffraction on crocoite powder with MoKα radiation (λ = 0.7093˚A). Recently, interesting behaviors have been reported for chromates when squeezed up to around 10 GPa[15 -22]. In particular, unusual isomorphic transitions have been detected in PbCrO3 (6 GPa) [17] and PbCrO4 (4 GPa) [21]. In the last compound, a second transition has been reported at 12 GPa[20]. Both transitions have been proposed to be correlated to changes in the electronic structure of $PbCrO_4$. The second transition produces a complete darkening of the sample, suggesting that probably it can be associated with a semiconductor-metal transition [21].

$PbCrO_4$ (the mineral crocoite) crystallizes at ambient pressure in the monoclinic monazite structure (space group *P21/n*, Z = 4). The structural arrangement of monazite is based on the nine-fold coordination of the Pb and the four-fold coordination of Cr[23]. Monazite-type oxides form an extended family of compounds. Because of their physical and chemical properties, several applications for these materials are already reported or under development [23-27]. These applications include photoconductive dielectric materials, humidity sensing resistors, yellow pigments, and effective solid lubricants. This list has been recently extended including applications as novel cathode materials for lithium-ion batteries [24], as green phosphors for light - emitting diodes [25] and in alternative green technologies [26-27]. Monazites exist in Nature and because of their incorporation of rare-earth elements they can effectively control the rare-earths distribution in igneous rocks [28-29]. In addition, they are a common accessory mineral in plutonic and metamorphic rocks. Therefore, the knowledge of the high-pressure (HP) behavior of monazites is very relevant not only for technological applications but also for mineral physics, chemistry, and petrology [31]. Because of the broad interest in monazite-type oxides, they have been lately extensively studied [32].

Interestingly, as in $PbCrO_4$, a similar isomorphic transition has been found under pressure in monazite-type $CeVO_4$ near 12 GPa[33]. In this case, the transition occurs together with a large drop of the electrical resistivity, which has been associated to a pressure-induced metallization. Therefore, it is clear that the study of the electronic properties of monazite oxides deserves some attention. Here, report a study of the optical and electronic properties of $PbCrO_4$ under compression. These properties have been explored by electrical transport and optical-absorption measurements.

Electronic-structure calculations have been also carried out. The low-pressure and the two high-pressure phases of $PbCrO_4$ have been characterized. All of them show a semiconductor behaviour, but a substantial narrowing of the band gap is detected upon compression

Resistivity measurements at room temperature were carried out up to 35 GPa using a "designer DAC" [34]. The pressure was measured by the ruby fluorescence technique were performed using high-purity polycrystalline samples obtained from Alfa-Aesar and no pressure medium. The resistance of $PbCrO_4$ was measured employing a standard DC four-probe technique with the four contacts separated by identical distance. The electrical resistivity (ρ) was estimated from the measured resistance (R) and the sample thickness (t) using equation $\rho = \pi t R / \ln 2$ [35].

Hall-effect and resistivity measurements under pressure up to 11 GPa were made with a 150 ton hydraulic press and steel-belted Bridgman tungsten carbide (WC) anvils [36-37]. Measurements were carried out in a Van der Pauw configuration. The samples were contained using two annealed pyrophyllite gaskets. Hexagonal boron nitride was used as pressure-transmitting medium and to electrically isolate the sample from the WC anvils. Samples were compact pellets made from high-purity $PbCrO_4$ powder obtained from Sigma-Aldrich. The pressure applied to the sample was calibrated against the transition pressures of calibrants[38].

The band-structure calculations were performed within the framework of density-functional theory, using the plane-wave pseudo-potential method as implemented in the VASP package [39-40]. The atomic species were described with projected-augmented wave (PAW) pseudo-potentials [41-42]. The exchange-correlation energy was taken in the generalized-gradient approximation (GGA) with the PBEsol prescription [43]. The plane-wave basis set employed extended up to an energy cutoff of 520 eV in order to have an accurate total-energy convergence of 1-2 meV per formula unit. Use a dense Monkhorst-Pack [44] grid appropriate to the structures considered to sample the Brillouin Zone (BZ), ensuring a high total-energy convergence. At each selected volume, the atomic positions and the unit-cell parameters were fully optimized. For the relaxed structure at the optimized configuration the atomic forces are smaller than 0.006 eV/Å, and the deviation of the stress tensor from a diagonal hydrostatic form is less than 0.1 GPa[45]. It is important to note that for each volume obtain the total energy as function of volume, but also

energy derivatives, like pressure as function of volume, are obtained from the stress tensor. Band-structure calculations have been carried out up to 12 GPa. They described the two monazite-type polymorphs that exist in this pressure range. Calculations at higher pressures were not performed because the crystal structure of $PbCrO_4$ beyond 12 GPa remains yet undetermined.

Due to the heavy mass of the Pb atoms, that also performed, at selected pressures, calculations of the electronic band structure including the spin-orbit (SO) coupling [46]. This greatly increases the computational time required for the simulations. However, from the results were concluded that the SO coupling effects do not appreciably affect the results obtained without including SO effects. Therefore, to evaluate the effect of pressure on the band structure of $PbCrO_4$ calculations were performed neglecting the SO interaction.

PbCrO₄ structure

Monoclinic structure, P21/n spacegroup (monazite).Used in pyrotechnic compositions,pigment, photocatalyst; also proposed as a laser host and they are highly toxic.A little-studied mineral need to explore.Is a semiconductor; structurally fine semiconductors have Eg=2.2 – 2.8 Ev ;Birefringence: δ=0.05; Value of E_g forcrocoite still unknown; theoretical value Eg~ 2.2 eV. Fig 5.1
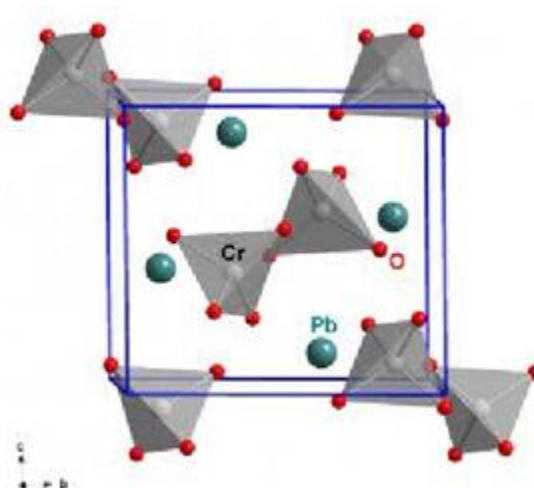

Figure PbCrO₄ structure

The structural arrangement is based on the nine - fold coordination of the A cation and the four - fold coordination of the X cation. Monazites exist in Nature and are important accessory minerals in granitoids and rhyolites, and because of their incorporation of rareearth elements they can effectively control the rare - earths distribution in igneous rocks [47].Monazite-type phosphates have been consequently studied under compression being the crystalline structure stable up to approximately 30 GPa. Cation substitution has seen shown to have a relevant influence on transition pressures in AXO_4oxides related to monazite. In particular, magnetic cations, like Cr, reduce considerably the transition pressures in Zircon-type oxides, favoring the study of HP phases. In this work, to gain further understanding of the structural properties of monazite-type oxides, HP x-ray diffraction, Raman, nd optical-absorption experiments on monazite-type $PbCrO_4$(the mineral crocoite) up to 18GPa re reported and detected the occurrence of two structural changes and characterized the structure of the HP phases. The equation of state (EOS) for different structures is presented too. Finally, lattice-dynamics properties and the electronic structure of $PbCrO_4$are studied

.The crystal structures, lattice vibrations, and electronic band structures of $PbCrO_4$, $PbSeO_4$, $SrCrO_4$, and $SrSeO_4$ were studied by ab initio calculations, Raman spectroscopy, X-ray diffraction, and optical-absorption measurements. Calculations properly describe the crystal structures of the four compounds, which are isomorphic to the monazite structure and were confirmed by X-ray diffraction. Information is also obtained on the Raman- and IR-active phonons, with all of the vibrational modes assigned. In addition, the band structures and electronic densities of states of the four compounds were determined. All are indirect-gap semiconductors. In particular, chromates are found to have band gaps smaller than 2.5 eV and selenates higher than 4.3 eV. In the chromates (selenates), the upper part of the valence band is dominated by O 2p states and the lower part of the conduction band is composed primarily of electronic states associated with the Cr 3d and O 2p (Se 4s and O 2p) states. Calculations also show that the band gap of $PbCrO_4$ ($PbSeO_4$) is smaller than the band gap of $SrCrO_4$ ($SrSeO_4$). This phenomenon is caused by Pb states, which, to some extent, also contribute to the top of the valence band and the bottom of the conduction band. The agreement between experiments and calculations is quite good; however, the band gaps are underestimated by calculations, with the exception of the bang gap

of SrCrO$_4$, for which theory and calculations agree. Calculations also provide predictions of the bulk modulus of the studied compounds.

Band gap in PbCrO$_4$

The Eg bandgap of the powders can be obtained by extrapolating relation (B) between 2.32 eV and 2.27 eV for PbCrO$_4$and 2.16 eV and 2.01 eV for Pb$_2$CrO$_5$. As can be seen, the band gap of powders decreases from 2.32 eV to 2.27 eV for PbCrO$_4$and from 2.16 eV to 2.01 eV for Pb$_2$CrO$_5$as the heat treatment increases from 400°C to 700°C. Elevating the treatment temperature, increase powder crystallinity and reduces band gap, thus increasing the conductive nature of compounds.

As described in Ref. [21], at ambient pressure were found that in PbCrO$_4$ the optical-absorption spectrum shows a steep absorption edge characteristic of a direct band gap. The determined value of the band-gap energy (Eg) at ambient pressure is 2.3 eV. Then followed the evolution with pressure of the absorption spectrum and determined the pressure dependence of Eg. At all pressures, the absorption spectra suggest that PbCrO4 remains being a direct gap semiconductor. The pressure evolution of Eg is shown in following Fig. found that upon compression the absorption edge gradually red-shifts up to a pressure close to 3 GPa. At 3.5 GPa, an abrupt change is detected, which produces a darkening of the red color of PbCrO$_4$.
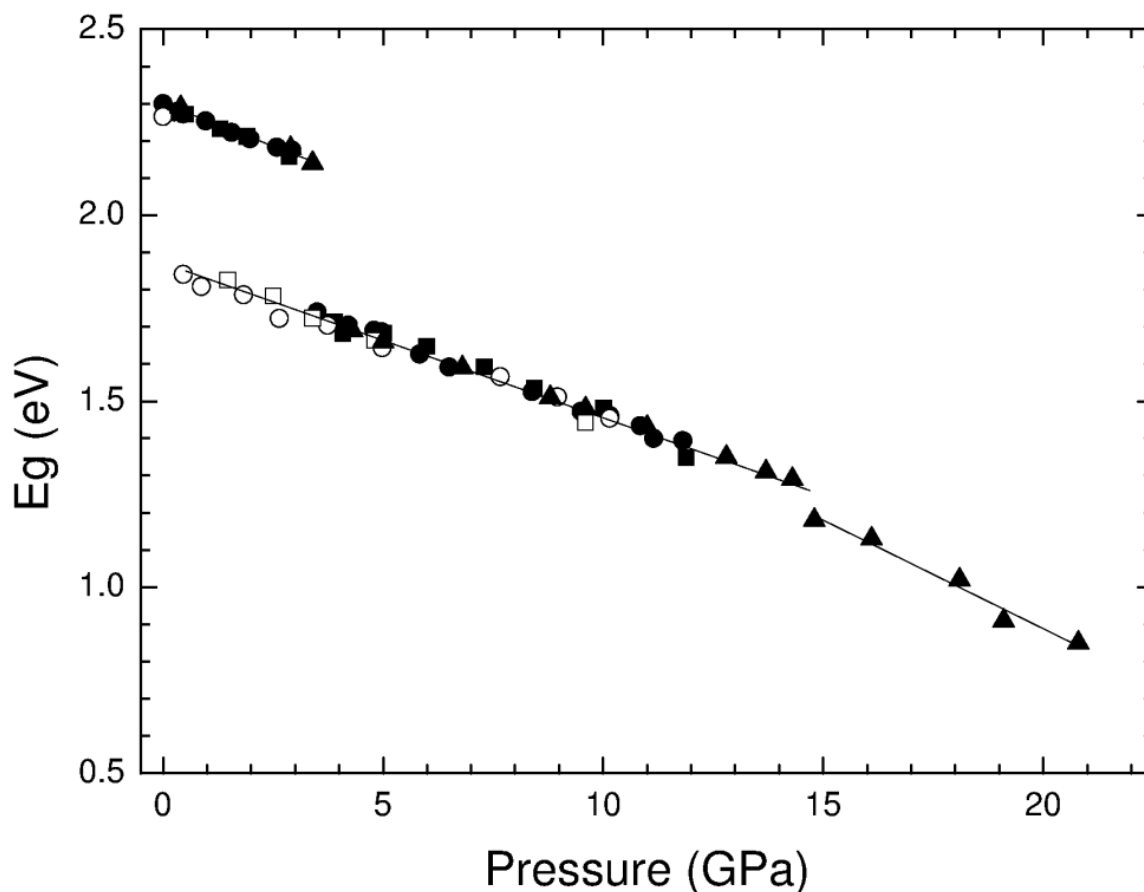
Fig. Pressure dependence of Eg. Symbols: experimental results corresponding to three independent experiments (triangles, circles, and squares). Solid symbols: upstroke. Empty symbols: downstroke. Lines are linear fits to the data.

This fact is caused by the occurrence of a 0.3 eV band-gap collapse above fig . As will explain when discussing calculations, this bang-gap change can be correlated with the isomorphic transition previously detected in $PbCrO_4$ by means of x-ray diffraction experiments (to a HP monazite-type structure). A similar transition has been also found in other monazites [48]. Beyond 3.5 GPa the pressure evolution of the absorption edge is also toward low energy. When pressure exceeds 12 GPa, the formation of defects in the $PbCrO_4$ crystal is detected. Beyond 14 GPa the crystal suddenly becomes black. This fact is in agreement with the occurrence of a second pressure-driven transition to a phase with an undetermined crystal structure. The blackening of $PbCrO_4$ is caused by the reduction of Eg to values smaller than 1.2 eV, without any evidence of metallization. From 15 to 21 GPa, Eg gradually decreases with pressure from 1.2 to 0.8 eV. In the three phases of $PbCrO_4$, the pressure

dependence of Eg can be well described by a linear function. The pressure coefficients, dEg/dP, are equal to 46 meV/GPa, -42 meV/GPa, and -60 meV/GPa, for monazite and the two subsequent HP phases, respectively. Changes induced by pressure in the absorption spectrum are reversible with a hysteresis that can reach up to 2 GPa. It is interesting to note that in the 21 GPa range covered by the experiments $PbCrO_4$ changes from having a band-gap energy similar to that of CdS at ambient pressure to having Eg similar to GaAs in the first HP phase and then having a narrow band gap like InN in the second HP phase.
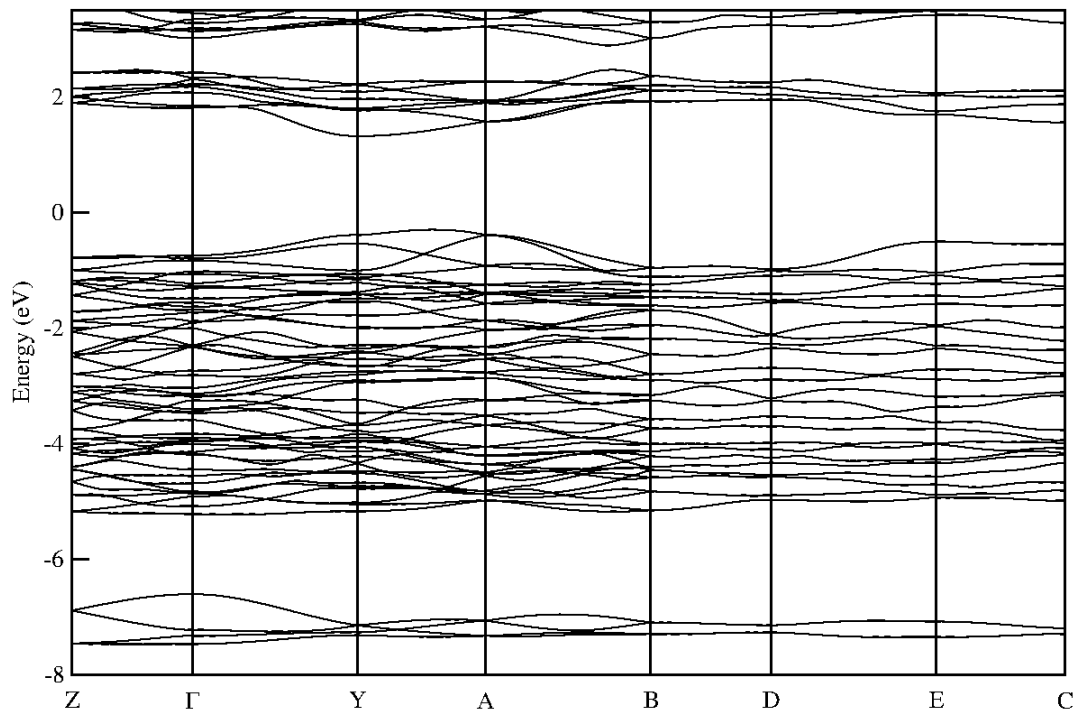
(A)
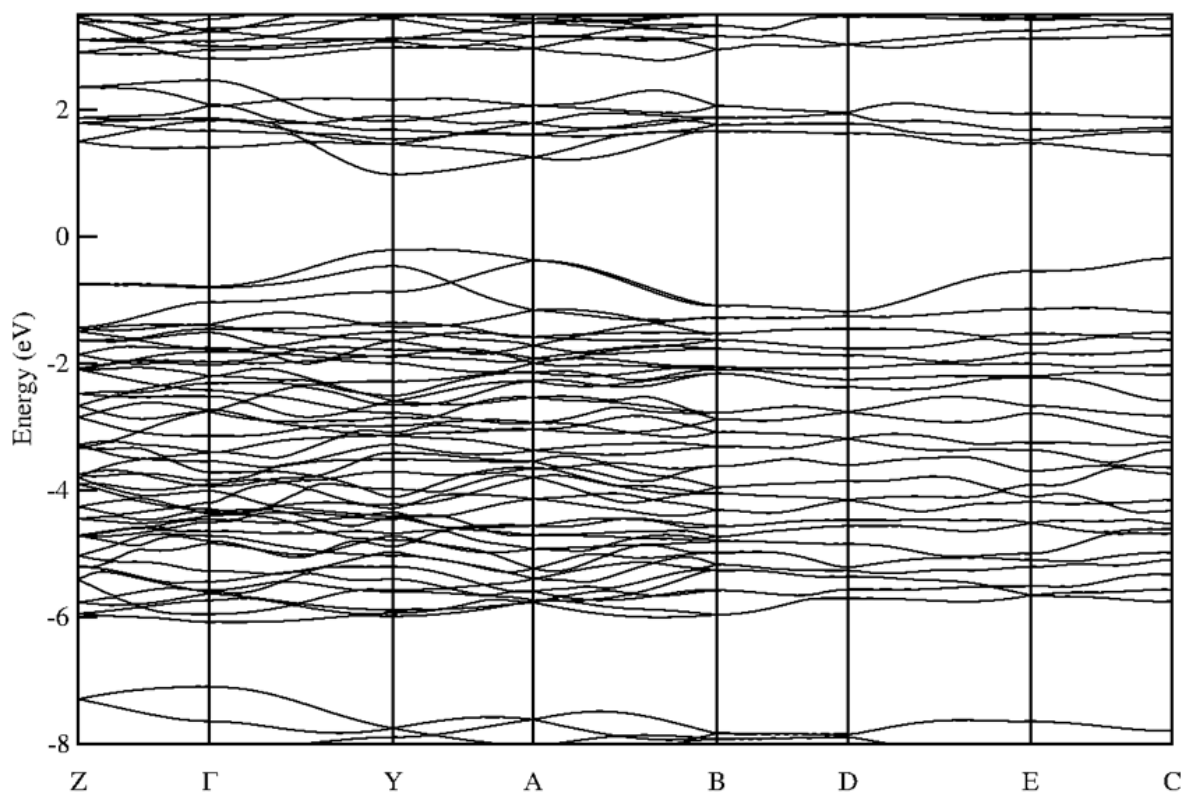
(B)

Fig. Calculated band structure of monazite-type $PbCrO_4$ and ambient pressure (top) and 8 GPa (bottom).

Discuss now the results of band-structure calculations in order to explain the behavior observed for Eg below 15 GPa. For the second HP phase such calculations were not carried out because the crystal structure of this phase has not been determined yet. For the calculated pressures, found that theory agree well with, providing a good description of the crystal structure at all the studied pressures. The calculated band structure and density of states (DOS) are shown in avobe Fig. At ambient pressure, calculations indicate that $PbCrO_4$ is an indirect band-gap material with the maximum of the valence band in between the Y and A points of the BZ and the minimum of the conduction band at the Y point. Calculations also established that the Y-Y direct band gap is 0.05eV higher than the indirect band gap. This fact is in apparent contradiction with experiments ($PbCrO_4$ behaves as a direct gap material). However the energy difference between the direct and indirect gap is small enough to make the indirect band gap undetectable by experiments because of the much higher absorption coefficient of the direct gap. The same apparent contrast between calculations and

experiments has been observed in monazite-type LaVO$_4$[49]. According to calculations, the value of Eg at ambient pressure is 1.3 eV. Therefore, Eg is underestimated by the calculations by 1 eV, as typically occurs with density-functional theory calculations [46]. However, these calculations provide an accurate description of the pressure evolution of Eg[50].
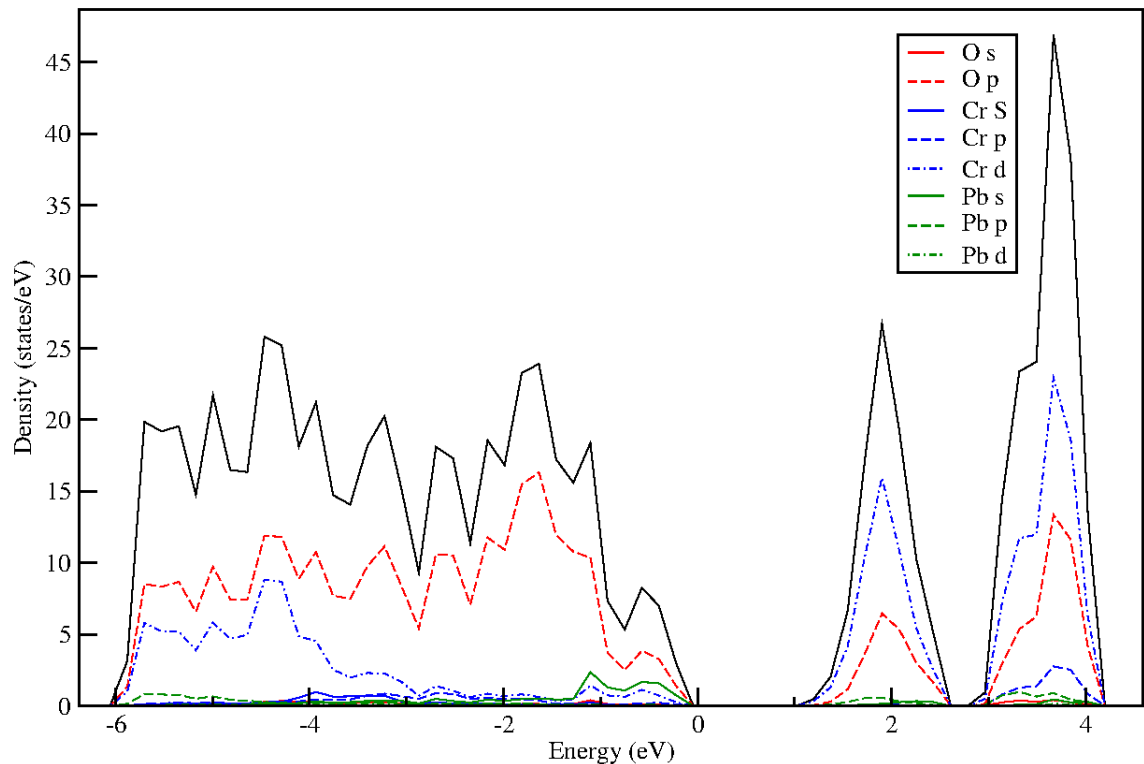

Fig. (color online) Calculated partial and total DOS of PbCrO$_4$. (top) low-pressure monazite at ambient pressure (bottom) high-pressure monazite at 8 GPa.

Pressure effects High

In above Fig it can be seen that at ambient pressure the main contribution to the bottom of the conduction band is coming from the hybridization between Cr^{3d} and O^{2p} orbitals (anti-bonding states). Pb $6p$ states have also a minimal contribution. On the other hand, the upper portion of the valence band is composed basically by the anti-bonding combination of the Pb $6s$ and O $2p$ states. According to our calculations, in the low-pressure phase, under compression the top of the valence band shifts toward high energies faster than the bottom of the conduction band. This is a

consequence of the fact that the application of pressure decreases the bond distances (in special Pb-O distances), thus increasing the orbital overlap. As a consequence of it, the separation between Pb bonding and anti-bonding states is enlarged. This fact enhances the displacement towards higher energies of the top of the valence band, but reduces the displacement of the bottom of the conduction band. This behavior is qualitatively similar to what is observed in PbWO4 [48]. It causes a reduction of the energy difference between the bottom of the conduction band and the top of the valence band, inducing the Eg reduction after observed in the experiments up to 3 GPa. Regarding, the band-gap collapse observed at 3.5 GPa, in agreement with experiments, calculations show that the isomorphic transition observed at the same pressure implies a 0.2 eV reduction of Eg. Although the isomorphic structural transition does not affect the global symmetry of the crystal, the crystal structure is highly distorted, affecting Cr-O and Pb-O bond angles and distances. These changes of the crystalline structure are reflected in the electronic structure of $PbCrO_4$, producing the small collapse of Eg that observed in the experiments. The changes in the electronic structure can be seen by comparing the band structure and DOS at ambient pressure and 8 GPa. In particular, after the transition the conduction band becomes broader. In addition, as observed in the experiments, calculations also found that the HP monazite-type phase has a nearly direct band gap at the Y point of the BZ. Regarding the pressure evolution of Eg in this phase, it is still as a first approximation controlled by the movement towards high energies of Pb 6s states. Because of that, after the transition, dEg/dP is similar to that of the low-pressure monazite-type phase.
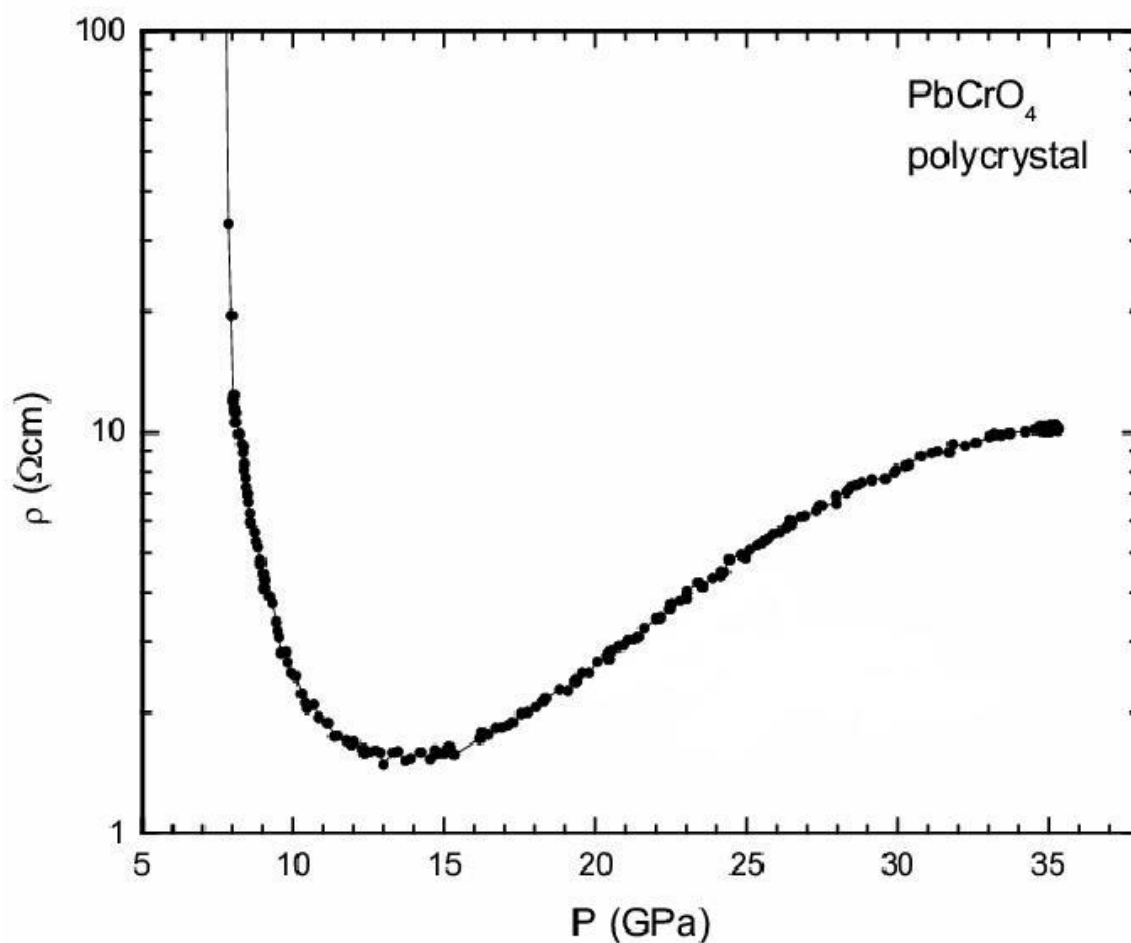
Fig. Resistivity as a function of pressure measured in the DAC.

Above Fig. shows the resistivity as a function of pressure for $PbCrO_4$ for DAC experiments. These measurements were limited to pressures larger than 8 GPa due to the high resistivity (> 100 MΩ) of the sample below this pressure, which compromise the accuracy of the transport measurements. From 8 to 12 GPa a two-orders of magnitude decrease of the resistivity is observed. A similar behavior is found in the resistivity of related monazite-type $CeVO_4$. The abrupt decrease of ρ is followed by a plateau between 11 and 14 GPa and a gradual increase of ρ from 14 to 35 GPa. The three pressure regions where the resistivity shows qualitatively different behaviors are consistent with the stability of the three phases of PbCrO4 determined from x-ray diffraction and Raman spectroscopy and with the three pressure regions determined from the band-gap behavior (see Fig. 5.1). An interesting fact to remark here is that PbCrO4 up to 35 GPa does not show resistivity values compatible with a pressure-

induced metallization. On the other hand, the gradual evolution of ρ beyond 14 GPa does not give any hint on the possible occurrence of any additional phase transition in $PbCrO_4$.
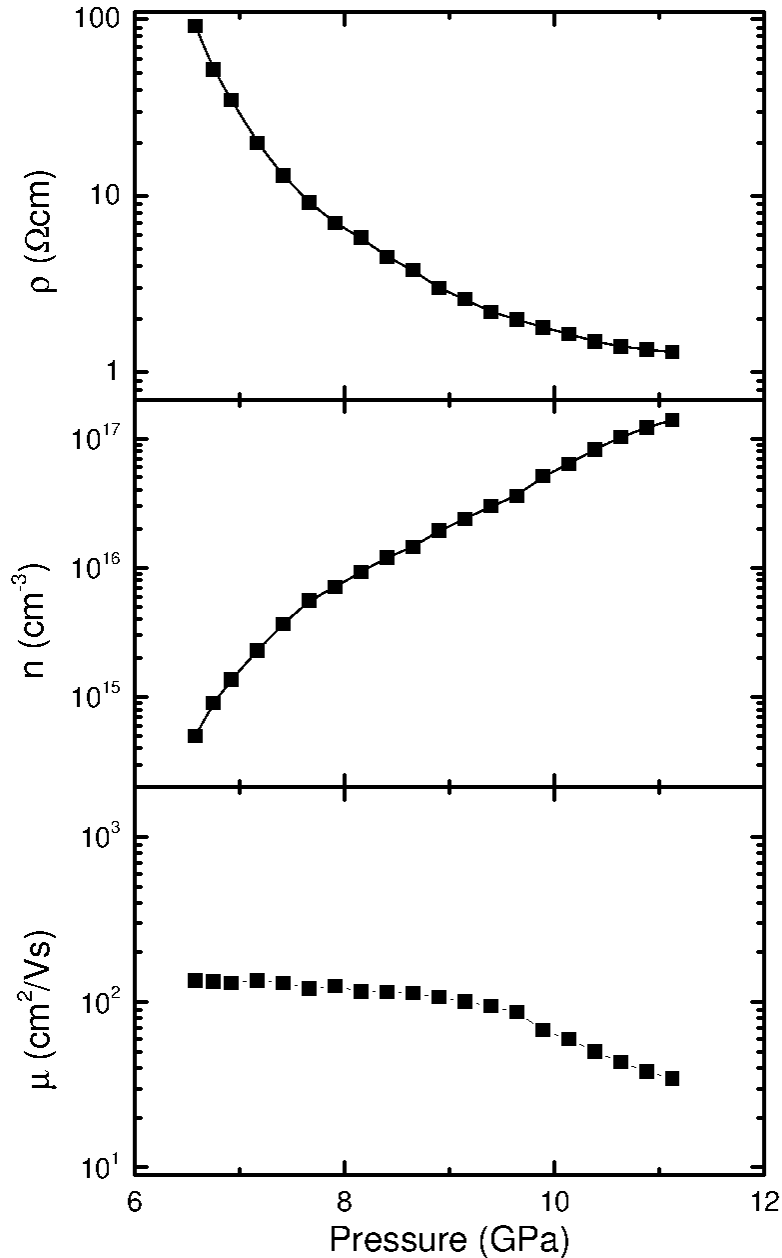

Fig. Resistivity, carrier concentration, and mobility as a function of pressure measured using large Bridgman anvils.

From above Fig. shows the resistivity (ρ), carrier concentration (n), and mobility (μ) measured in PbCrO4 as a function of pressure from 7 to 11 GPa (i.e. when the HP

monazite-type phase is stable). Measurements at lower pressure cannot be performed accurately due to the high resistivity of $PbCrO_4$. They were not possible at higher pressure due to limitations of the experimental set up within the explored pressure range $PbCrO_4$ behaves as an n-type semiconductor. This fact agrees with the semiconductor behavior found in monazite-type $LaCrO_4$[52]. The carrier concentration monotonically increases with pressure and the mobility gradually decreases up to 9.5 GPa, decreasing considerably more beyond this pressure. The reduction of ρ under compression is then mainly due to the increase of n.

Before discussing the physical reasons of the results described above, that would like to remark the fact that in the three experiments here described different pressure-transmitting medium were used (16:3:1 methanol-ethanol-water, hexagonal BN, and no pressure medium).

Now pass to discuss the possible origin of the carrier concentration observed in $PbCrO_4$. The smallest value observed for it is four orders of magnitude larger than the intrinsic concentration for such band-gap range at ambient pressure. Therefore, it is reasonable to assume that the HP phase of PbCrO4 behaves like an extrinsic semiconductor with donor levels. It is know that oxygen vacancy formation is typical in monazite-type oxides [53-54]. Basically, oxygen migrates from its lattice position to an interstitial site. It creates a vacancy defect at its original site and an interstitial defect at its new location (Frenkel defect). The vacancy could probably behave as a deep donor. This phenomenon has been observed in related oxides [55] where doubly ionized oxygen vacancies and interstitials lead to an n-type semiconductor behavior. In the case of PbCrO4, that, as in other compounds [56], the pressure-induced (isomorphic) transition could lead to the creation of a large concentration of donor centers that makes the material to behave as an extrinsic n-type semiconductor. In particular, if one defect is introduced per unit-cell, the concentration of donors can be estimated to have a maximum value of 31021 cm^{-3}, more than enough for creating the measured carrier concentration. Under this hypothesis, let us discuss if the increase found for the carrier concentration can be explained by a decrease of the activation energy of the donors.

Given the existence of Frenkel pairs the material would necessarily contain some compensating acceptors. For a non-degenerate compensated n-type semiconductor, in the low-temperature limit

$$n = N_C \frac{N_D - N_A}{2N_A} e^{\frac{-\Delta E_D}{kT}}$$

where NC is the effective density of states of the conduction band, ND (NA) is the donor (acceptor) concentration, T is the absolute temperature, k is the Boltzmann constant, and ΔED = EC - ED is the ionization energy of the donor level (being EC the energy minimum of the conduction band and ED

the energy of the donor level). From this expression, if the change in the effective density of states is neglected, from the exponential increase of n under pressure can easily deduce that

$$\frac{\partial \ln n}{\partial P} = -\frac{1}{kT} \frac{\partial (E_C - E_D)}{\partial P}$$

From the logarithmic slope of the pressure dependence to determine the pressure coefficient of the donor level ionization energy, that turns out to be about 23meV/GPa, which leads to a decrease of some 115 meV in the donor ionization energy in the range from 6 to 11 GPa. Given that the band gap in the first high-pressure phase decreases with a pressure coefficient of -42 meV/GPa, the relative decrease of the band gap in the same pressure interval would be about 13%. The k.p model [46] would predict an overall relative reduction of the electron effective mass by around 13%, leading to the same decrease in the ionization energy of a shallow donor that would not be enough to give account of the observed decrease of the ionization energy. A deep-to-shallow transformation in the nature of the donor level seems more likely as the origin of the large increase of n. This kind of effect is not uncommon in semiconductors and is related to changes induced by pressure in the relative position of different conduction-band minima . The same ionized impurity center gives rise to impurity levels with different ionization energies whose relative position in the band gap depends on the electron effective mass in the corresponding conduction-band minimum. The above described shallow-to-deep donor transformation will drive an increase of the number of ionized donor impurities under pressure leading to the

detected increase in n (and the consequent decrease in ρ). The picture described above, which should be confirmed by combined HP-HT transport measurement [56], provides not only a plausible explanation to the observed behavior of the carrier concentration, but also is consistent with the changes observed in μ. Both facts indicate that it is reasonable model. In particular, the decrease observed for the mobility is consistent with the increase of the ionized impurities concentration leading to an enhancement of electron scattering by ionized donors [58]. The change of slope at about 9.5 GPa would correspond to the change of the dominant scattering mechanism. Below 9.5 GPa phonon scattering is dominant and μ slowly decreases due to the increase of the impurity scattering contribution. Between 9.5 GPa and 11 GPa the mobility decreases by a factor 3, while n increases by the same factor. This indicates that ionized impurity scattering becomes dominant and μ decreases as the inverse of the impurity concentration.

Regarding the increase observed in ρ at the second phase transition (near 15 GPa), it cannot be related to changes in the band structure and the activation energy of donors. Note that Eg is further reduced after the second transition reaching values smaller than 1 eV. A reasonable argument to explain the upturn of ρ is that the second phase transition induced by pressure creates a highly defective crystal. This assumption is consistent with the fact that black defects in the crystal can be visually detected in the pressure range where the onset of the increase of ρ is found (as described above). Indeed, the density of defects rises upon compression and the sample becomes polycrystalline. Carrier trapping and scattering at the grain frontiers can easily induce a decrease in μ. It can also produce a partial compensation of the semiconductor reducing consequently n. Both facts will favor the increase of the resistivity shown in Fig. 5.5 This hypothesis is consistent with the fact that defect creation has been found to be the cause of pressure-induced resistivity increases in materials with a small band gap [57] (like the second HP phase of PbCrO4).

Conclusions

The transport and optical properties of PbCrO4 have been explored under compression by means of resistivity, Hall-effect, and optical-absorption measurements as well as band-structure calculations. PbCrO4, a direct band-gap semiconductor with Eg = 2.3 eV, undergoes changes in its electronic properties associated to pressure-induced structural transitions. In particular, at 3.5 GPa a

collapse of Eg is detected, which correlates well with a decrease of resistivity and with an isomorphic structural phase transition. Up to the second transition, PbCrO4 behaves as an n-type semiconductor with a donor level. The origin of this level is proposed to be associated to the formation of oxygen vacancies. Upon compression the donors apparently transform from deep to shallow levels producing an increase of the carrier concentration and the observed decrease of ρ. After the second transition (~ 15 GPa) Eg becomes smaller than 1.2 eV. In this phase the resistivity increases as pressure does probably due to the self-compensation of the donor levels and the increase of electron scattering by ionized donors. In the three phases the band gap red shifts under compression. At 20 GPa, Eg is approximately 0.8 eV, so PbCrO4 behaves as a narrow-gap semiconductor. Such a large change of the electronic band gap in a reduced pressure range is associated to the presence of anti-bonding Pb states in the top of the valence band. In spite of the large decrease of Eg induced by pressure, no evidence of metallization is detected in PbCrO4 up to 35 GPa. The conclusions extracted from this study are quite useful for the application of PbCrO4 to selective hydrogen combustion, which open up opportunities for developing energy-efficient oxidative dehydrogenation routes to commercial important olefins [50]. Expect the interesting reported results will probably trigger future studies.

References

1. C. Burda, X. B. Chen, R. Narayanan, M.A. El-Sayed. Chem. Rev. **105** (2005) 1025-1102.
2. T. L. Porter, M. E. Hagerman, B. P. Reynolds, M. P. Eastman, R. A. Parnell, J. Polym. Sci. Part B-Polym. Phys. **36** (1998) 673-679.
3. H. Cölfen, S. Mann. Angew. Chem., Int. Ed. **42** (2003) 2350-2365.
4. S. R. Dickinson, K. M. McGrath. J. Mat. Chem. **13** (2003) 928-933.
5. K. Toda, S. Watanabe. J. Mat. Sci. Lett. **18** (1999) 689-690.
6. N. Yukami, M. Ikeda, Y. Harada, M. Nisitani, T. Nishikura. IEEE Trans. Electron Dev. **33** (1986) 520-525.
7. W. W. Wang, Y. J. Zhu. Cryst. Growth Des. **5** (2005) 505-507.
8. K. A. Wishah, M. M. Abdul-Gader. Appl. Phys. A: Mater. Sci. Process. **66** (1998) 229-234.
9. A. K. Panda, B. B. Bhowmik, A. R. Das, S. P. Moulik. Langmuir **17** (2001) 1811-1816.

10. J. Liang, Y. Li, J. Cryst. Growth **261** (2004) 577-580.

11. X. L. Hu, Y. J. Zhu, Chem. Lett. **33** (2004) 880-881.

12. D. Chen, K. Tang, Z. Liang, Y. Liu, H. Zheng, Nanotechnology **16** (2005) 2619-2624.

13. Y. J. Zhu, W. W. Wang, R. J. Qi, X. L. Hu, Angew. Chem., Int. Ed. **43** (2004) 1410-1414.

14. J. H. Xiang, S. H. Yu, Z. Xu, Cryst. Growth Des. **4** (2004) 1311-1315.

15. R. Vidya, P. Ravindran, P. Vajeeston, H. Fjellvåg, and A. Kjekshus, Phys. Rev. B 72 (2005) 014411.

16. Y. W. Long, L. X. Yang, S. J. You, Y. Yu, R. C. Yu, C. Q. Jin, and J. Liu, J. Phys.: Condens. Matter 18 (2006) 2421- 2428.

17. W. Xiao, D. Tan, X. Xiong, J. Liu, and J. Xu, Proc. Nat. Acad. Sci. 107 (2010) 14026 - 14029.

18. E. ClimentPascual, J. M. Gallardo Amores, R. SáezPuche, M. Castro, N. Taira, J. Romero de Paz, and L. C. Chapon, Phys. Rev. B 81 (2010) 174419.

19. D. Errandonea, R. Kumar, J. Lopez-Solano, P. Rodrıguez-Hernandez, A. Muñoz, M. G. Rabie, and R. SaezPuche, Phys. Rev. B 83 (2011) 134109.

20. D. Santamarıa-Perez, R. S. Kumar, A. J. Dos santos-Garcıa, D. Errandonea, R. Chulia-Jordan, R. Saez-Puche, P. Rodrıguez-Hernandez, and A. Muñoz, Phys. Rev. B 86 (2012) 094116.

21. E. Bandiello, D. Errandonea, D. Martinez-Garcia, D. Santamaria-Perez, and F. J. Manjón, Phys. Rev. B 85 (2012) 024108.

22. D. Santamaría-Pérez, E. Bandiello, D.Errandonea, J. Ruiz-Fuertes, O. Gomis, J. A. Sans, F. J. Manjón, P. Rodriguez-Hernandez, A. Muñoz, J. Phys. Chem. C 117 (2013) 12239 - 12248.

23. N. Clavier, R. Podor, and N. Dacheux, J. Eur. Ceram. Soc. 31 (2011) 941 - 976.

24. B. Hu, X. Wang, Q. Wei, H. Shu, X. Yang, Y. Bai, H. Wu, Y. Song, and L. Liu, J. Alloys Compd. 579 (2013) 18 - 26.

25. K. Park and M. H. Heo, J. Alloys Compd. 509 (2011) 9111 – 9115.

26. D. Errandonea, F. J. Manjon, A. Muñoz, P- Rodriguez-Hernandez, V. Panchal, S. N. Achary, and A. K. Tyagi, J. Alloys Compd. 577 (2013) 327 – 335.16

27. Y. Zhang, G. Li, H. Yang, Z. Lu, and R. Chen, J. Alloys Compd. 551 (2013) 544 – 550.

28. A. Meldrum, L. A. Boatner, and R. C. Ewing, Phys. Rev. B 56 (1997) 13805 - 13814.

29. R. Lacomba-Perales, D. Errandonea, Y. Meng, and M. Bettinelli, Phys. Rev. B 81 (2010) 064113.

30. D. Rubatto, J. Hermann, and I. S. Buick, J. Petrol. 47 (2006) 1973 - 1996.

31. H. Li, H. M. Noh, B. K. Moon, B. C. Choi, and J. H. Jeong, J. Allos Compd. 582 (2014) 151 – 156.

32. S. N. Achary, D. Errandonea, A. Muñoz, P. Rodríguez-Hernández, F. J. Manjón, P. S. R. Krishna, S. J. Patwe, V. Grover, and A. K. Tyagi, Dalton Trans. 42 (2013) 14999 -15015

33. A. B. Garg, K.V. Shanavas, B.N. Wani, and S.M. Sharma, J. Solid State Chem. 203 (2013) 273 - 280 .

34. D. D. Jackson, J. R. Jeffries, W. Qiu, J. D. Griffith, S. McCall, C. Aracne, M. Fluss, M. B. Maple, S. T. Weir, Y. K. Vohra, Phys. Rev. B 74 (2006) 174401.

35. X. Huang, C. Cao, Y. Han, M. Li, C. He, A. Hao, D. Zhang, C. Yui, G. Zou, and Y. Ma, Appl. Phys. Lett. 90 (2007) 242102.

36. D. Errandonea, A. Segura, D. Martínez-García, and V. Muñoz-San Jose, Phys. Rev. B 79 (2009) 125203.

37. D. Errandonea, J. Appl. Phys. 108 (2010) 033517.

38. D. Errandonea, D. Martinez-Garcia, A. Segura, J. Ruiz-Fuertes, R. Lacomba-Perales, V. Fages, A. Chevy, L. Roa, and V. Muñoz, High Press. Res. 26 (2006) 513 - 518.

39. G. Kresse and J. Hafner, Phys. Rev. B 47 (1993) 558 - 561.

40. G. Kresse and J. Furthmüller, Phys. Rev. B 54 (1996) 11169 - 11186.

41. G. Kresse and D. Joubert, Phys. Rev. B 59 (1999) 1758 - 1775.

42. P. E. Blochl, Phys. Rev. B 50 (1994) 17953 - 17979.

43. J. P. Perdew, A. Ruzsinszky, G. I. Csonka, O. A. Vydrov, G. E. Scuseria, L. A. Constantin, X. Zhou, and K. Burke, Phys. Rev. Lett. 100 (2008) 136406.

44. H. J. Monkhorst and J. D. Pack, Phys. Rev. B 13 (1976) 5188 - 5192.

45. A. Mujica, A. Rubio, and A. Muñoz, Rev. Mod. Phys. 75 (2003) 863 - 912.

46. P. Yu and M. Cardona, *Fundamentals of Semiconductors*, 2nd Edition, Springer-Verlag (Berlin-Heidelberg-New York, 2003).

47. T. Huang, J.-S. Lee, J. Kung, and C.-M. Lin, Solid State Communications 150 (2010) 1845 - 1850.

48. D. Errandonea, C. Popescu, S. N. Achary, A. K. Tyagi, and M. Bettinelli, to appear in Mater. Research Bulletin (2013).18

49. L. Sun, X. Zhao, Y. Li, P. Li, H. Sun, X. Cheng, and W. Fan, J. Appl. Phys. 108 (2010) 093519.

50. J. Ruiz-Fuertes, S. Lopez-Moreno, J. Lopez-Solano, D. Errandonea, A. Segura, R. Lacomba-Perales, A. Muñoz,S. Radescu, P. Rodrıguez-Hernandez, M. Gospodinov, L. L. Nagornaya, and C. Y. Tu, Phys. Rev. B 86 (2012) 125202.

51. D. Errandonea, D. Martınez-Garcıa, R. Lacomba-Perales, J. Ruiz-Fuertes,and A. Segura, Appl. Phys. Lett. 89 (2006) 091913.

52. Y. Aoki, H. Konno, and H. Tachikawa, J. Mater. Chem. 11 (2001) 1214 - 1218.

53. T. S. Bjorheim, T. Norby, and R. Haugsrud, J. Mater. Chem. 22 (2012) 1652 - 1661.

54. M. L. Williams, M. J. Jercinovic, and C. J. Hetherington, Annu. Rev. Earth Planet. Sci. 35 (2007) 137 - 175.

55. C. M. C: Vera and R. Aragon, J. Solid State. Chem. 181 (2008) 1075 - 1079.

56. D. Errandonea, A. Segura, J. F. Sanchez-Royo, and V. Muñoz, P. Grima and A. Chevy, and C. Ulrich, Phys. Rev. B 55 (1997) 16217 - 16225.

57. D. Errandonea, A. Segura, F. J. Manjon, and A. Chevy, Semicond. Sci. Technol. 18 (2003) 241 - 246.

58. W. Walukiewicz, Phys. Rev. B 41 (1990) 10218 - 10220.